Lasers in Surgery and Medicine 25:159–169 (1999)

Optical Phantom Materials for Near Infrared Laser Photocoagulation Studies

Megumi N. Iizuka, MSc,[1] Michael D. Sherar, PhD,[1] and I. Alex Vitkin, PhD[1,2]*

[1]Ontario Cancer Institute and Department of Medical Biophysics, University of Toronto, Toronto, Ontario M5G 2M9, Canada
[2]Department of Radiation Oncology, University of Toronto, Toronto, Ontario M5G 2M9, Canada

Background and Objective: **Phantoms were developed that simulate tissue with dynamic and static optical properties with which to study the effects of laser irradiation.**
Study Design/Materials and Methods: **Albumen, agar, and an absorbing dye (Naphthol Green) were combined to form a phantom with heat sensitive optical properties to mimic tissue response. The optical properties of this phantom were measured by using the added absorber technique. A polyacrylamide phantom with static optical properties was designed with the equivalent values of μ_a and μ_s' by combining appropriate concentrations of Naphthol Green and Intralipid-10%.**
Results: **The absorption and reduced scattering coefficient of the phantoms were 0.50 ± 0.04 cm^{-1} and 2.67 ± 0.07 cm^{-1} respectively, in the native state at 805 nm. In the coagulated state, the absorption and scattering coefficient were 0.7 ± 0.1 cm^{-1} and 13.1 ± 0.5 cm^{-1} respectively.**
Conclusion: **Two phantoms with dynamic or static optical properties were developed with properties similar to tissue. They may be used in future studies of opto-thermal effects in tissues. Lasers Surg. Med. 25:159–169, 1999.**

Key words: albumen; agar; naphthol green; polyacrylamide; Intralipid; poison moderator; added absorber; phantoms; NIR; opto-thermal

INTRODUCTION

The use of tissue-equivalent materials (phantoms) for opto-thermal biomedical laser applications provides a means for investigating the propagation and absorption of light and subsequent temperature rise in tissue. As such, they are valuable for testing theoretical models, which predict the response of tissue during laser irradiation causing thermal damage such as interstitial laser photocoagulation (ILP). Using actual tissue may be impractical due to the constraints of accessibility and storage of fresh samples. Reproducibility of results may also be poor because of the difficulty in finding identical specimens. Furthermore, preparation of the sample may change the properties of the tissue specimen. Nevertheless, thermal measurements have been made in tissue samples [1,2]. An alternative approach is to use tissue-equivalent materials or phantoms. Phantoms are usually homogeneous, and therefore do not normally possess the complex structures that exist throughout tissue such as the vasculature and stroma. Therefore, tissue substitutes do not necessarily reflect the true complexity and hence response of tissue during laser therapy. However, they do provide a qualitative means of testing the parameters and assumptions made in mathematical models and may indicate generally important features of opto-thermal processes in tissue.

Phantoms may also be used to demonstrate

Contract grant sponsor: National Cancer Institute of Canada.

*Correspondence to: Dr. Alex Vitkin, Ontario Cancer Institute, Room 7-415, 610 University Avenue, Toronto, Ontario M5G 2M9, Canada. E-mail: vitkin@oci.utoronto.ca

Accepted 25 March 1999

and elucidate the transient effects of interstitial laser heating. For example, heating of tissue during ILP produces a coagulated region surrounded by healthy tissue. This occurs in a dynamic fashion, which depends upon a variety of factors such as the temperature dependent changes in optical properties of the tissue and changes in blood perfusion. The dynamic responses of tissues to these parameters are not yet well understood. Phantoms may therefore be used to investigate these effects in a controlled fashion where the complexities of in vivo studies can be avoided. The phantom discussed specifically in this article simulates the dynamic response of tissue due to thermally-induced changes in optical properties alone.

Many tissue-equivalent materials have been proposed for use in optical applications such as spectroscopy and imaging [3–10]. Unfortunately, most of these phantoms are liquid, making them a poor choice for thermal dosimetry phantom studies due to convection. Other have used collagen gels [10], polyacrylamide gels [11], and albumen [12] to observe the effects of laser ablation. Ablation induces vapourization with short laser pulses (picoseconds to milliseconds) causing mechanical damage. The biophysical mechanisms of ablation and their measurement methods differ greatly from those of photothermal responses. Few phantoms have been proposed specifically for photothermal studies. Some investigators have examined the possibility of using ex vivo tissue as a phantom material for this purpose [13–15]. However, ex vivo tissue may require additional preparation such as homogenization [13,14] and may not have the same optical properties as living tissues due to the absence of oxygenated blood [16].

Egg white (albumen) has been studied and proposed as an alternative material for use in studies of laser irradiation [12,17–19]. It is a convenient material, since it is readily available, reproducible, homogeneous, and uniform in appearance. Furthermore, it responds to heat in a similar manner to tissue in that it undergoes a visible irreversible whitening effects as a result of thermal coagulation.

Albumen is comprised mainly of globular proteins (about 10.2%), lipids (0.05%), and water (88.1%) [17]. Albumen powder is available commercially and is composed of dehydrated egg white. Exposure to heat causes an unfolding of the albumen proteins, which then precipitate out of solution and rapidly form aggregates [17]. Consequently, albumen visibly whitens during this process, which is quantified by an increase in the reduced scattering coefficient μ_s' [17,19]. In its native state, albumen absorbs weakly and has a low scattering coefficient in the near infrared (NIR) relative to biological tissues [17]. To achieve optical properties that are more closely matched to tissue, we propose adding a dye to increase absorption and a polysaccharide gel (agar or agarose) to increase the scattering and to stiffen the phantom. Naphthol Green is an effective absorber of short near infrared (NIR) wavelengths (700–850 nm). Agar acts as a solidifying agent making it more conducive to thermal measurements of bulk specimens.

The optical properties of this phantom were measured with the added absorber technique, which is based upon diffusion theory [20,21]. The added absorber technique has been used previously to measure the optical properties of bovine liver, bovine muscle, pig brain, and chicken muscle [21]. It is employed in highly scattering tissue by adding increasing concentrations of dye of known absorption and measuring the extent of light penetration in these samples. The absorber can be uniformly combined with the albumen solution to provide a homogeneous mixture.

A second phantom was developed to act as a control medium whose optical and thermal properties do not change with temperature. A control phantom can be used to demonstrate the difference in opto-thermal predictions when heat-induced changes in optical properties are not accounted for. Polyacrylamide was used as a base material due to its high melting point [11]. The liquid monomer undergoes an exothermic reaction and solidifies upon addition of a catalyst, producing a pliable, yet structurally supportive rubber-like gel. The material has also been used as a muscle-equivalent phantom for hyperthermia with microwave and radio frequency electromagnetic waves [22].

Polyacrylamide is suitable as an optical phantom as it is transparent in the NIR. The water based solution of liquid-phase acrylamide can be doped with absorbing dyes and scattering materials to obtain the desired optical properties. An ideal phantom uses a non-scattering absorbing medium and a non-absorbing scattering medium [5]. Naphthol Green was used as a NIR absorber because this organic powder is highly water soluble [23] and thus introduces minimal scattering in the polyacrylamide solution. An example of an effective scatterer for use in phantoms is Intralipid-10%. This is a white liquid emulsion of 10% solution of soybean oil in water. The soybean

oil exists as phospholipid micelles in suspension, which give Intralipid-10% its scattering properties [7]. This material has been previously studied and well characterized [6,7]. These studies indicate that Intralipid is weakly absorbing and can be diluted to produce a scattering coefficient that is very similar to that of tissue in the NIR.

MATERIALS AND METHODS

Added Absorber Technique

Theory. The optical properties of the albumen phantom were determined by the added absorber technique, also known as the poisoned moderator method of neutron transport physics [20,21]. This technique involves the measurement of the effective attenuation coefficient of tissue, μ_{eff}, which is defined as [24]:

$$\mu_{eff} = \sqrt{3\mu_a \cdot (\mu_a + \mu_s')} \quad (1)$$

where μ_a is the absorption coefficient in tissue and $\mu_s' = \mu_s(1 - g)$ is the reduced scattering coefficient. The factor, g, is the anisotropy factor, which describes the effects of directionally dependent anisotropic scattering [25]. Equation (1) is obtained from solving the light diffusion approximation for diffuse fluence rate, ϕ. The fluence rate for an isotropic point source radiator in spherical coordinates is proportional to:

$$\phi(r) \propto \frac{exp(-\mu_{eff} r)}{r} \quad (2)$$

A complete derivation of equations (1) and (2) is available in various texts [24]. The added absorber technique measures the effective attenuation coefficient of different samples doped with increasing concentrations of absorber. The absorption coefficient is equal to the total absorption of the dye and the medium. Therefore, the effective attenuation coefficient given in equation (1) expands to

$$\mu_{eff}^2 = 3 \cdot [\mu_{ap} + \mu_{ad}'] \cdot ([\mu_{ap} + \mu_{ad}'] + \mu_{sp}') \quad (3)$$

where μ_{sp} equals the scattering coefficient of the phantom and μ_{ap}, μ_{ad} are equal to the absorption coefficient of the phantom and the dye respectively. For media where scattering events occur much more frequently than absorption events, it can be assumed that $(\mu_{ap} + \mu_{ad}) << \mu'_{sp}$. Thus, equation (3) simplifies to:

$$\mu_{eff}^2 \simeq 3 \cdot (\mu_{ap} + \mu_{ad}) \cdot (\mu_{sp}') \simeq 3\mu_{ap}\mu_{sp}' + 3\mu_{ad}\mu_{sp}' \quad (4)$$

This also assumes, implicitly, that the scattering coefficient does not change due to the presence of the added dye.

Equation (4) demonstrates that the scattering and absorption coefficient of the phantom (μ_{sp}' and μ_{ap}') can be determined from the slope and intercept of the plot of μ_{eff}^2 vs. μ_{ad}. [Note that eq. (3) can also be solved using second order quadratic curve fitting tools. However, to simplify our analysis, a straight line fit was used.] The effective attenuation, μ_{eff}, was obtained experimentally by measuring the fluence as a function of depth and applying equation (2). A range of values of the independent variable, μ_{ad}, was obtained by doping samples of albumen phantoms with different quantities of dye of known absorption coefficient. The optical properties of the phantom were determined at a wavelength of 805 nm with this technique. This is a common wavelength for laser-induced coagulation applications such as ILP.

Measurement apparatus and method. The fluence rate of the albumen samples was measured in a Plexiglass box with inner dimensions of 6 × 6 × 6 cm (Fig. 1). The source fiber was a commercially available optical fiber with a spherical diffusing tip (Pseudosphere, Rare Earth Medical, West Yarmouth, Massachusetts), which acts as an isotropic point source. The diameter of the fiber tip was 1.5 mm. The dosimetry probe was constructed from a 600 μm plane cut end fiber. The method of construction is explained in appendix A.

The source fiber was held in place by a 14 gauge needle, which was inserted through a hole at the center of one side of the box. The source fiber was placed such that the diffusing tip extended beyond the sharp end of the needle. A shortened 14 gauge needle was secured through a second hole on the opposing face. The dosimetry probe was inserted into this second needle and held in place by a small piece of plastic tubing. The tubing acted as a sleeve that centered the fiber portion within the short needle. The axes of the source and sensing probes were aligned by visual inspection. Outside the box, the dosimetry fiber was attached to a micrometer controlled translation stage (Thorlab, Newton, New Jersey) used to measure the distance between the optical source and dosimetry probe.

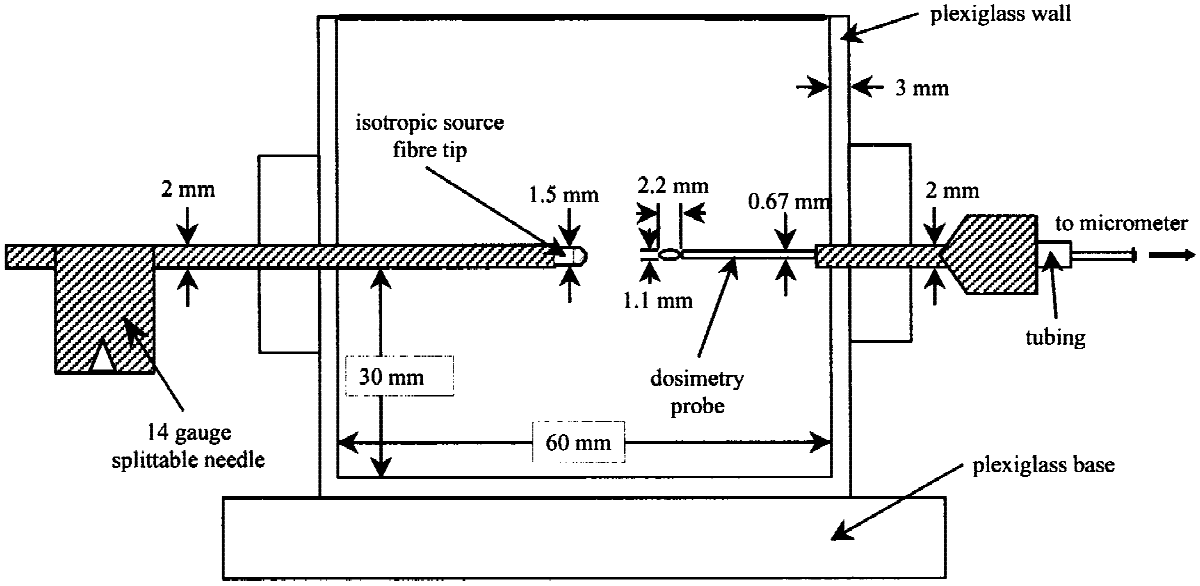

Fig. 1. Schematic diagram of apparatus used to measure fluence rate as a function of radial distance.

Testing of the fluence box set-up was performed by measuring the absorption coefficient of different concentrations of dye solutions in water. The absorption coefficient of the samples was confirmed independently with spectrophotometer measurements.

The albumen phantom and the doped samples of increasing added absorber concentrations were previously solidified in six individual Plexiglass molds with the same dimensions as the fluence box apparatus. The first albumen phantom was removed from its mold and placed in the box. The source needle was inserted into the sample. The isotropic fiber tip was then fed inside the needle and was exposed at the sharp tip of the needle. The fiber was coupled to a NIR 805 nm laser diode (Diomed-15, Diomed Ltd., Cambridge, UK) via an SMA 905 connector. The end of the dosimetry probe fiber was directed at a silicon photodetector (PDA50, Thorlab). The detector output, displayed on a voltmeter, was proportional to the fluence [26]. On the lowest power laser setting (500 mW), the dosimetry tip was moved toward the source fiber using the translation stage over a distance of approximately 0.5 cm to 1.5 cm. The micrometer scale, r, and the photodetector voltages, V, (which is proportional to the fluence, ϕ) were recorded every 0.5 to 1 mm. The effective attenuation coefficient was determined by plotting $ln(V \cdot r)$ vs. r in accordance with the prediction of equation 2. The sample was removed and returned to its original mold.

The radial fluence measurement was repeated for the doped albumen samples. The original phantom and the doped samples were then heated together in a large water bath at 85°C for 45 minutes. The albumen fluence rate measurements were performed again in a different set of tracks for the albumen phantoms in the coagulated state. The optical properties of the albumen were determined in accordance with equation (4) as a function of the added absorber concentration values listed in Table 1.

Albumen Phantom Design

The albumen phantom consisted of chicken egg albumen (Crude, Grade II, Sigma, St. Louis, USA), bacteriological agar (Agar #1, Oxoid, Hampshire, England) and Naphthol Green dye (Sigma). The phantom was constructed by combining two mixtures: a stock albumen solution and an agar-dye solution.

Stock solution of albumen was prepared by dissolving 22.2% by weight powdered egg white in 77.8% by weight distilled water. This was filtered through a fine mesh strainer producing a translucent, homogeneous, yellow liquid, which was refrigerated when not in use. Table 1 lists the composition of six agar solutions that were prepared individually. Each solution contained agar, dye, and water. The dye was prepared in advance, as a stock solution, which increased the ease of use and also ensured consistent levels of dye concentrations from sample to sample. The stock solution consisted to 0.387 g of Naphthol Green dis-

TABLE 1. Composition of Albumen Phantom and Samples*

Added μ_a (/cm)	Naphthol Green (% by weight)	Distilled water (% by weight)
0.00	13.3	32.0
0.32	18.6	26.7
0.64	23.9	21.3
1.96	29.2	16.0
1.28	34.5	10.7
1.60	39.8	5.4

*The first row is the composition of the albumen phantom. The other rows are the absorber doped samples used in determining the optical properties of the phantom by using the added absorber technique. 1.4% (by weight) agar powder and 53.3% (by weight) albumen stock are combined with the distilled water and Naphthol Green solution. The albumen stock consisted of 22.2% by weight albumen powder and 77.8% by weight water. Density of albumen phantom ≈1.01 g/mL.

solved in 1 L of distilled water to give a 0.0387% (by volume) dye concentration. A spectrophotometer (UV160, Mandel Scientific Co. Ltd, Guelph, Canada) was used to measure the spectral absorption of this dye at this concentration, which was equal to 5.9 cm^{-1} at 805 nm, the wavelength of our laser source.

The dye concentrations were calculated such that the absorption coefficient increased by 0.32 cm^{-1} between successive samples. The ultimate phantom (base phantom), for which the optical properties were determined, contained the lowest dye concentration. The other albumen samples (doped samples) were prepared with increasing added absorber concentrations of dye to determine the optical properties of the base phantom. The agar solution was prepared by combining the dye and distilled water, which was heated to approximately 70°C. The agar powder was slowly added and dissolved until the boiling point (85°C) of the mixture was reached. The solution was cooled in a warm water bath to about 45°C. As the agar formula cooled, the albumen stock solution was warmed in a hot water bath to approximately 40°C. The albumen was then added to the cooled agar solution and mixed thoroughly with a spatula. Cooling the agar prevented it from coagulating the albumen on contact, whereas heating the albumen avoided uneven gelling and bubble formation within the agar solution. The phantom was then poured into a mold and allowed to cool. The phantom solidified at 38°C and reached room temperature after approximately 2 hours of cooling. This process was repeated for all the dye concentrations listed in Table 1.

TABLE 2. Composition of Acrylamide Stock Solution

Component	Stock (% by weight)
Acrylamide	26.00
N,N′-methylenebisacrylamide	0.20
Sodium chloride	1.05
De-ionized water	72.75

Polyacrylamide Phantom Design

A second set of control phantoms were made with polyacrylamide gel. They were used to demonstrate the thermal response with static optical properties. Control phantoms were designed to match the optical properties of the albumen in the native and in the coagulated states, by adding appropriate amounts of dye and scattering solution.

The design of the polyacrylamide gel phantom was based upon the phantom developed by Surowiec et al. for a tissue-equivalent phantom for microwave applicators [22]. This phantom was prepared from an aqueous solution of monomer acrylamide and a cross-linking reagent, N,N′-methylenebisacrylamide. The original phantom design also includes the addition of sodium chloride to simulate the electrical conductivity of tissue. The polymerization process is initiated upon addition of the catalysts, ammonium persulfate (APS) and TEMED. This results in an exothermic reaction producing a pliable yet structurally supportive rubber-like gel, which molds to the shape of the containment vessel. The phantom can be preserved for several months in this state, as long as it is refrigerated and sealed within plastic wrap to prevent drying.

As recommended by Surowiec et al., a preparation solution of gel stock solution was used from which subsequent phantoms were produced. The stock solution consisted of the acrylamide, the crosslinking reagent (N,N′-methylenebisacrylamide), sodium chloride, and water without the polymerization catalysts (APS and TEMED) (see Table 2).

To match the optical properties with that of albumen, the dopants, Naphthol Green and Intralipid-10% were added to the liquid-phase solution of polyacrylamide (acrylamide). The Naphthol Green was a 0.210% by volume solution with an absorption coefficient of 32.3 cm^{-1} at 805 nm measured with the spectrophotometer. Polyacrylamide was formed by reacting the solution with the catalysts, TEMED and a 10% solution of ammonium persulfate, causing exothermic polymer-

ization. With the addition of the catalysts, the solution was mixed vigourously for approximately 1 minute and poured into the mold. The solidification process began after approximately 5 minutes after the addition of the catalyst. The phantom was completely polymerized after a period of about 2 hours. Cooling of the sample required an additional 3 to 4 hours.

Initial attempts at combining the acrylamide with the dye, resulted in a visible photochemical bleaching reaction between the ammonium persulfate and the dye, which was manifested as a fading of the green colour of the sample during the polymerization process. To quantify the bleaching phenomenon, the absorption coefficient of purely absorbing samples were measured with the spectrophotometer, 1 minute, 2 hours, and 24 hours after reacting the acrylamide with the catalyst.

The scattering coefficient of acrylamide was determined by varying concentrations of Intralipid-10% with a fixed concentration of dye of known μ_a. The resultant effective attenuation coefficient, μ_{eff}, of the samples in the liquid phase was measured in the same fluence box apparatus used for measuring the optical properties in the albumen phantom. The samples were measured while in their liquid phase before polymerization or bleaching occurred. From these curves μ_s' was calculated from the known value of μ_a and the measured value of μ_{eff} by applying equation (1).

The final effective attenuation coefficients of acrylamide phantoms were examined in liquid acrylamide samples with the addition of both Intralipid-10% and dye. They were compared with the fluence rates as a function of radial distance of that measured in the native and coagulated albumen phantoms.

RESULTS

The fluence box apparatus was designed to measure radial fluence to determine the optical properties of the phantoms. Unfortunately, test samples of known absorbing and scattering properties at 805 nm were unavailable. Therefore, testing of the apparatus could only be performed on purely absorbing materials, which could then be independently confirmed with spectrophotometer results. Four dye samples of known absorption coefficients were tested in the fluence box with the source and sensing probes. The absorption coefficients measured in the apparatus were compared with spectrophotometer results at 805 nm (see Fig. 2). There was good agreement between the two measurement sets.

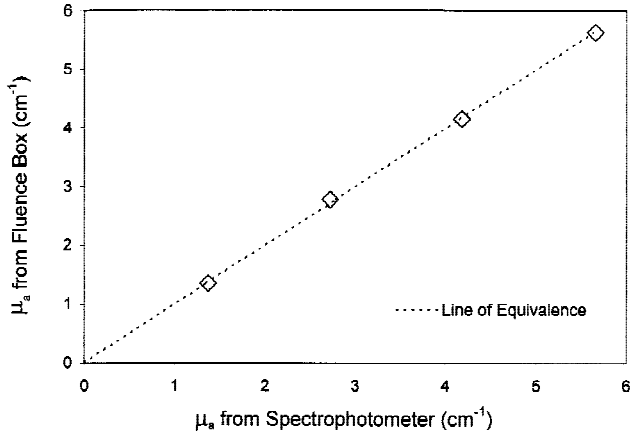

Fig. 2. Absorption coefficients of dye samples at 805 nm, experimentally determined from radial dependence of fluence (using the slope of $\ln[V \cdot r]$), compared with spectrophotometer results. Concentration of dye samples: 9.5, 19.1, 28.6, and 38.2 $\mu g \cdot l^{-1}$.

The fluence profiles of the albumen phantom and the added absorber samples with added dye were measured in the fluence box apparatus to determine the optical properties of the albumen phantom by using the added absorber moderator technique. Figures 3 and 4 show the radial fluence rate plots for the native and coagulated states of the phantom respectively. The effective attenuation coefficient of the phantom in the two states was calculated from the slopes of these curves. The square of the effective attenuation as a function of added absorber is plotted in Figure 5. The optical properties of the original (i.e., no absorber added) albumen phantom were calculated from the slope and intercept of this plot using equation (4). The optical properties of the albumen are shown in Table 3. There was a 1.4 fold increase in μ_a and a 4.9 fold increase in μ_s' from the native to coagulated states.

Control polyacrylamide phantoms were designed to match the optical properties of the albumen in the native and coagulated states, by adding appropriate amounts of dye and scattering solution. The effect of bleaching of the dye with ammonium persulfate during the polymerization process of acrylamide was examined. The absorp-

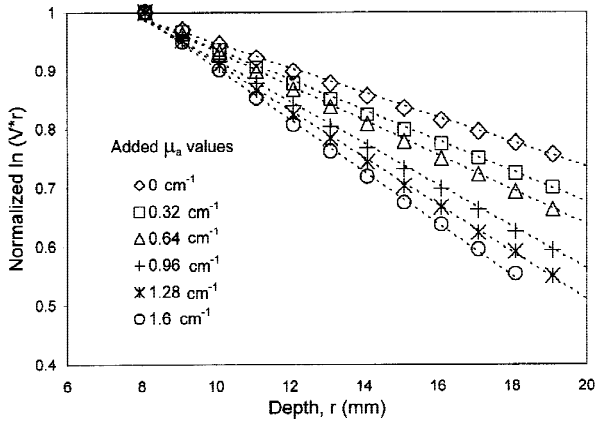

Fig. 3. Fluence rate as a function of radial distance for the base albumen phantom and the doped samples in the native state. The lines represent the linear fit.

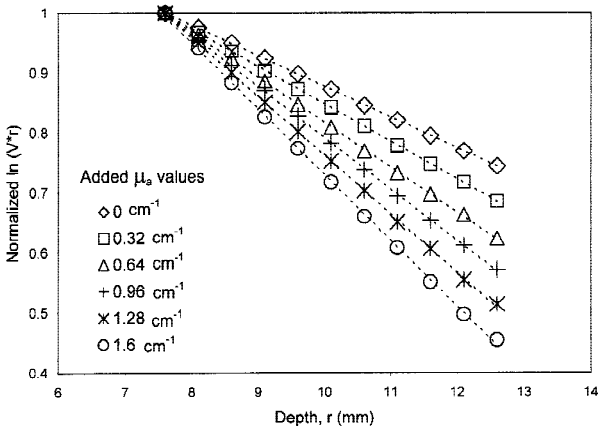

Fig. 4. Fluence rate as a function of radial distance for the base albumen phantom and the doped samples in the coagulated state. The lines represent the linear fit.

tion coefficient of phantoms with four different dye concentrations, measured at 1 minute, 2 hours, and 24 hours after the addition of the catalysts to the liquid acrylamide is shown in Figure 6. A drop in absorption due to the photochemical bleaching process is seen. There was no further change in absorption after 2 hours. By interpolating between the points of the final lower absorption curve, the percent mass concentrations of dye solution required to match the native and coagulated properties of the albumen phantoms were calculated to be 7.81% and 8.95% respectively. These values are recorded in Table 4.

The scattering coefficient of the Intralipid-10% in the polyacrylamide phantom was calculated from μ_{eff} [equation (1)] and plotted against the concentration of Intralipid by percent weight

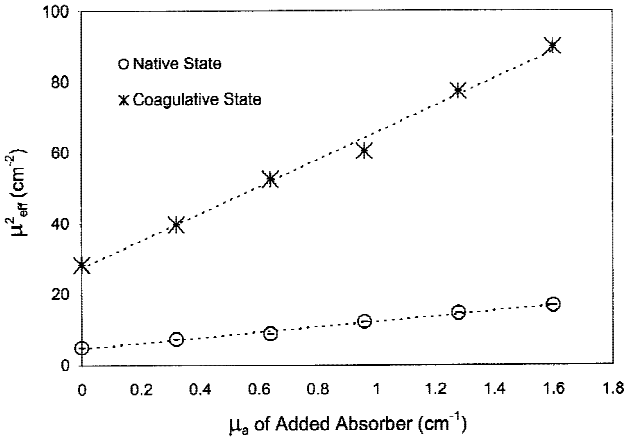

Fig. 5. Plot of μ_{eff}^2 against added absorber μ_a used to determine the optical properties of the albumen base phantom. The lines represent the linear fit. The standard error of the fitted slopes and intercepts produce the calculated error in the estimated optical properties.

TABLE 3. Optical Properties of the Albumen Phantom

State	μ_a (cm^{-1})	μ_s' (cm^{-1})	μ_{eff} (cm^{-1})
Native	0.50 ± 0.04	2.67 ± 0.07	2.2 ± 0.2
Coagulated	0.7 ± 0.1	13.1 ± 0.5	5.3 ± 0.6

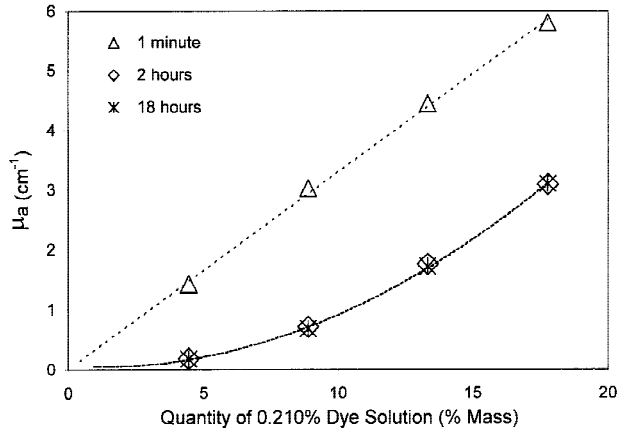

Fig. 6. The absorption coefficient of acrylamide before and after polymerization measured by spectrophotometer.

in Figure 7. This plot indicates that the scattering coefficient was proportional to the concentration of scattering material. By interpolating between the points of this curve, the percent concentration of Intralipid was determined to be 4.40% and 22.53% to match the native and coagulated scattering coefficients of the albumen phantom respectively. The final composition of the polyacryl-

TABLE 4. Final Composition of Polyacrylamide Phantom

Component	Matching native state albumen (% by weight)	Matching coagulated state albumen (% by weight)
Naphthol Green (0.210%)	7.81	8.95
Intralipid-10%	4.40	22.53
Distilled water	40.16	20.91
Acrylamide stock[a]	46.63	46.63
APS (10% by volume)	0.65	0.65
TEMED	0.35	0.35

[a]See Table 2.

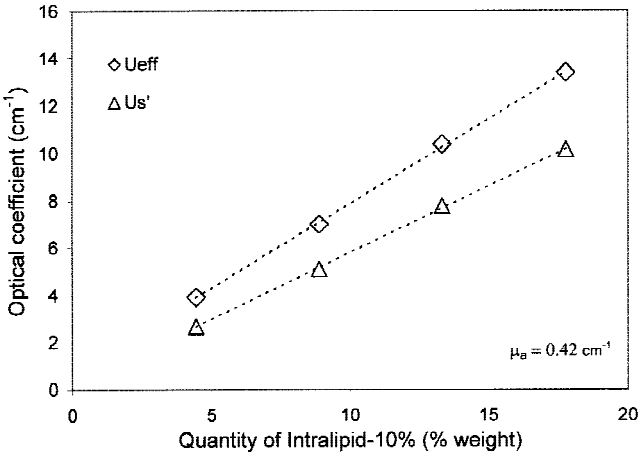

Fig. 7. The μ_s' and μ_{eff} of polyacrylamide samples with varying concentrations of Intralipid-10%. The lines represent the linear fit.

amide phantoms is summarized in Table 4. The predicted effective attenuation coefficients of the polyacrylamide phantoms are in good agreement with the albumen phantom properties as shown in Figure 8.

DISCUSSION

The μ_a and μ_s' in the native state of the albumen phantom (0.50 ± 0.04 cm^{-1} and 2.67 ± 0.07 cm^{-1}) and in the coagulated state (0.7 ± 0.1 cm^{-1} and 13.1 ± 0.5 cm^{-1}) are similar to values for tissue. For example, measurements on human prostate at 850 nm yielded μ_a = 0.6 cm^{-1} and μ_s' = 6 cm^{-1} in the native state and μ_a = 0.7 cm^{-1} and μ_s' = 13.8 cm^{-1} in the coagulated state [27]. Hence, the phantoms developed in this article may be useful for simulating ILP treatments in tissue and testing opto-thermal models of ILP.

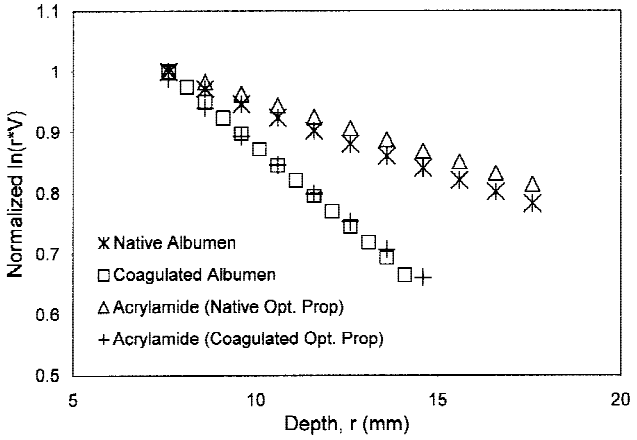

Fig. 8. Comparison of the fluence rates between the albumen and doped acrylamide phantoms.

The practical advantages of the albumen phantom are numerous. It is non-toxic, simple to make, easily poured into molds, and cost efficient. It can also be sliced or carved to any shape, and produces clearly visible zones of thermal coagulation to the naked eye. Furthermore, the absorbing dye is photochemically stable in the NIR wavelengths over several months. A small disadvantage is that it must be refrigerated and is recommended for use for only 1–2 weeks.

Polyacrylamide phantoms were developed whose optical properties do not change with temperature. This phantom provides a reference set of measurements to illustrate the difference in temperature predictions when heat-induced changes in optical properties are not accounted for. The optical properties of the phantoms were matched with those of the albumen phantom in both states by adding appropriate concentrations of Naphthol Green and Intralipid-10%. The transparent nature of polyacrylamide allows one to dope it to produce a wide range of tissue like optical properties, by varying the concentration of dye and scattering materials. We have demonstrated that the optical properties could then be experimentally determined and verified using fluence measurements and light diffusion theory.

Like the albumen phantom, polyacrylamide also offers many advantages. It is simple to make, easily poured into molds and cost efficient. Advantages of polyacrylamide over tissue phantoms are that it can be stored for several months, it is homogeneous, reproducible, and clean to work with. A problem with the polyacrylamide phantom was the effect of the catalyst, APS, on the

absorption characteristics of Naphthol Green. This resulted in a bleaching effect that had to be compensated for by increasing the initial concentration of dye. Furthermore, as shown in Figure 6, the bleaching effects were dependent upon the concentration of dye added. Also, polyacrylamide in its monomeric phase is a toxin. Therefore, safety handling procedures must be employed prior to polymerization.[1]

Another problem with the polyacrylamide phantom was that the fluence rate measurements have to be performed while the phantom was in its liquid unpolymerized form. The reason for this is that movement of the dosimetry probe in this solid polymerized form is very difficult. The inability to measure fluence of the phantom in its polymerized state leads to some uncertainty in the final scattering characteristics of the polyacrylamide phantom. Changes in the orientation and/or position of the scattering particles may occur due to settling of the Intralipid during the polymerization process. Other possible effects due to polymerization include the change in the index of refraction of the polymerized state and/or changes due to a chemical reaction with the catalysts or other base materials. The influence of these errors, however, appear to be minimal. This was confirmed by measuring the temperature rise in the polyacrylamide phantom in the solidified state and comparing it to theoretical predictions that used the calculated optical properties. Good agreement between predicted and experimental values suggest that the polymerization process does not significantly affect the optical properties.

It may be important to note that Intralipid-10% may interact with Naphthol Green influencing the scattering properties of the Intralipid-10% itself. The exact nature of the interaction between the two materials can only be speculated upon since this information is not readily available. Hence, an alternative design is the use of polystyrene sphere as a scattering agent. Polystyrene spheres have been successfully shown to provide predictable scattering properties in phantoms [4]. Therefore, characterization with this material is recommended for future phantom designs. However, one drawback of polystyrene spheres as compared to Intralipid is their high cost.

For opto-thermal studies, such as ILP, the phantoms should have thermal properties, and optical properties that are similar to tissue. The thermal properties of the albumen and polyacrylamide phantoms were not measured. However, since the albumen material is completely organic and consists mostly of water, the thermal properties are likely to be similar to that of tissue. The polyacrylamide phantom, though synthetic, may also be similar to tissue since it is composed mostly of water. The thermal properties can be estimated according to water content [28], which has previously shown high accuracy for other water based materials such as gelatine [29]. In future studies, however, the thermal properties of these phantoms should be measured.

[1]Once polymerized, polyacrylamide is safe to handle [22].

CONCLUSIONS

Two material systems were developed and characterized that possess either dynamic optical properties (albumen phantom) or constant optical properties (polyacrylamide phantom). A detailed procedure for phantom preparation and optical properties determination was presented. The optical properties of the albumen phantom were measured in both its native and coagulated states, and were then matched by the static polyacrylamide phantoms. The results were similar to tissue optical properties at 805 nm. As such they may be used in future investigations that study the opto-thermal response of tissue due to laser irradiation.

ACKNOWLEDGEMENTS

The authors thank Dr. Brian Wilson and Dr. Lothar Lilge for helpful discussions and technical assistance. This work was supported by a grant from the National Cancer Institute of Canada with funds from the Terry Fox Run. M.N.I. was partially supported by the Jack R. Cunningham Fellowship of the Ontario Cancer Institute.

REFERENCES

1. Xu LX, Chen MM, Holmes KR, Arken H. The theoretical evaluation of the Pennes, the Chenholmes and the Weinbaum-Jiji bioheat transfer models in the pig renal cortex. Advances in biological heat and mass transfer. ASME 1991; HTD-Vol. 189/BED-Vol. 18:15–21.
2. Prapavat V, Roggan A, Walter J, Beuthan J, Klingbeil U, Muller G. In vitro studies and computer simulations to assess the use of a diode laser (850 nm) for laser-induced thermotherapy (litt). Lasers Surg Med 1996;18:22–33.
3. Firbank M, Delpy DT. A design for a stable and reproducible phantom for use in near-infrared imaging and

spectroscopy. Physics in Medicine and Biology 1993;38: 847–853.
4. Firbank M, Oda M, Delpy DT. An improved design for a stable and reproducible phantom material for use in near-infrared spectroscopy and imaging. Physics in Medicine and Biology 1995;40:955–961.
5. Royston DD, Poston RS, Prahl SA. Optical properties of scattering and absorbing materials used in the development of optical phantoms at 1064 nm. Journal of Biomedical Optics 1996;1(1):110–116.
6. Flock ST, Jacques SL, Wilson BC, Star WM, van Gemert MJC. Optical properties of intralipid: a phantom medium for light propagation studies. Lasers Surg Med 1992;12: 510–519.
7. Staveren HJ, Moes CJM, van Marie J, Prahl SA, van Gemert MJC. Light scattering in intralipid-10% in the wavelength range of 400–1100 nm. Applied Optics 1991;30(31):4507–4514.
8. Kohl M, Essenpreis M, Cope M. The influence of glucose concentration upon the transport of light in tissue-simulating phantoms. Physics in Medicine and Biology 1995;40(7):1267–1287.
9. Wagnieres G, Cheng S, Zellweger M, Utke N, Braichotte D, Ballinni J, vanden Bergh H. An optical phantom with tissue-like properties in the visible for use in PDT and fluorescence spectroscopy. Physics in Medicine and Biology 1997;42:1415–1426.
10. Oraevsky AA, Jacques SL, Esanaliev RO, Tittel FK. Pulsed laser ablation of soft tissues, gels, and aqueous solutions at temperatures below 100°C. Lasers Surg Med 1996;18:231–240.
11. LeCarpentier GL, Motamedi M, McMath LP, Rastegar S, Welch AJ. Continuous wave laser ablation of tissue: analysis of thermal and mechanical events. IEEE Transactions on Biomedical Engineering 1993;40(2):188–200.
12. Halldorsson T, Langerholc J, Senatori L, Funk H. Thermal action of laser irradiation in biological material monitored by egg-white coagulation. Applied Optics 1981;20(5):822–825.
13. Whelan WM, Wyman DR, Wilson BC. Investigations of large vessel cooling during interstitial laser heating. Medical Physics 1995;22(1):105–115.
14. Wyman DR, Swift CL, Siwek RA, Wilson BC. A control method for a nonlinear multivariable system: application to interstitial laser hyperthermia. IEEE Transactions on Biomedical Engineering 1991;38(9):891–898.
15. Suzuki T, Kurokawa K, Higashi H, Suzuki K, Yamanaka H. Transurethral balloon laser enhanced thermotherapy in the canine prostate. Lasers Surg Med 1997;21:321–328.
16. Welch AJ, van Gemert MJC, Star WM, Wilson BC. Definitions and overview of tissue optics. In: Welch AJ, van Gemert MJC, editors. Optical thermal response of laser-irradiated tissue. New York: Plenum Press; 1995. p 15–46.
17. Pickering JW. Optical property changes as a result of protein denature in albumen and yolk. Journal of Photochemistry, Photobiology and B: Biology 1992;16:101–111.
18. Yang Y, Welch AJ, Rylander III HG. Rate process parameters of albumen. Lasers Surg Med 1991;11:188–190.
19. Meijerink R, Essepreis M, Pickering JW, Massen CH, Mills TN, van Gemert MJC. Rate process parameters of egg white measured by light scattering. In: Müller G, Roggan A, editors. Laser-induced interstitial thermotherapy. Bellingham, Washington: SPIE Press; 1995.
20. Wilson BC. Measurement of tissue optical properties: Methods and theories. In: Welch AJ, van Gemert MJC, editors. Optical-thermal Response of Laser-irradiated Tissue. New York: Plenum Press; 1995.
21. Wilson BC, Patterson MS, Burns DM. Effect of photosensitizer concentration in tissue on the penetration depth of photoactivating light. Lasers in Medical Science 1986;1: 235–244.
22. Surowiec A, Shrivastava PN, Astrahan M, Petrovich Z. Utilization of a multilayer polyacrylamide phantom for evaluation of hyperthermia applicators. International Journal of Hyperthermia 1992;8(6):795–807.
23. Sigma Chemical Company. Technical sheets on Naphthol Green. 1998.
24. Star WM. Diffusion theory of light transport. In: Welch AJ, van Gemert MJC, editors. Optical-thermal response of laser irradiated tissue, chapter 6. New York: Plenum Press; 1995. p 131–205.
25. Wyman DR, Patterson MS, Wilson BC. Similarity relations for the interaction parameters in radiation transport and their applications. Applied Optics 1989;28: 5243–5249.
26. Thorlab. PDA50-amplified silicon detector. Thorlab, Newton, New Jersey.
27. Roggan A, Dörschel K, Minet O, Wolff D, Müller G. The optical properties of biological tissue in the near infrared wavelength range—review and measurements. In: Müller G, Roggan, A, editors. Laser-induced interstitial thermotherapy. Bellingham, Washington: SPIE Press; 1995. p 10–44.
28. Takata AN, Zaneveld L, Richter W. Laser-induced thermal damage in skin. Technical Report SAM-TR-77-38, USAF School Aerospace Med., 1977.
29. Duck FA. Physical properties of tissue, complete reference book. London, England: Academic Press; 1990.
30. Wyman DR, Whelan WM, Wilson BC. Interstitial laser photocoagulation: Nd:YAG 1064 nm optical fiber source compared to point heat source. Lasers Surg Med 1992; 12:659–664.

APPENDIX:

Dosimetry Probe Design

To measure the light fluence rate, an isotropic dosimetry probe with a scattering spherical tip was constructed from a 600 μm plane cut end fiber. The polished, cut end of the fiber was embedded to a depth of ≈3 mm into a mixture of titanium dioxide particles (TiPure, C35R4, Dupont, Wilmington, Delaware) and epoxy, which cures under ultraviolet (UV) light (J91 Epoxy, Summerslab Corporation). The fiber was coupled via lens to a helium cadmium laser, which emits in the ultraviolet range. Using low laser power, the light

propagated down the fiber and illuminated the epoxy mixture at the cut end of the fiber. In the presence of the scattering material, the cut end radiates in a quasi-isotropic fashion [30]. Therefore, the epoxy cures in a spherically symmetric fashion around the fiber tip. After 4 hours of irradiation, the cured end was removed from the epoxy mixture. The outside of the tip was then placed under a UV lamp for an additional 2 hours.

The isotropy of the dosimetry probe was measured by irradiating the tip externally with collimated laser light beam from the 805 nm laser diode used in this study. The light entering the dosimetry probe was detected at the distal end by a photodetector. The fluence was measured as a function of incident angle by rotating the collimated beam around the probe in the plane parallel to the axis of the fiber.

The normalized polar plot of the detected fluence from a collimated beam as a function of angle in the plane parallel to the axis of the fiber is shown in Figure 9.

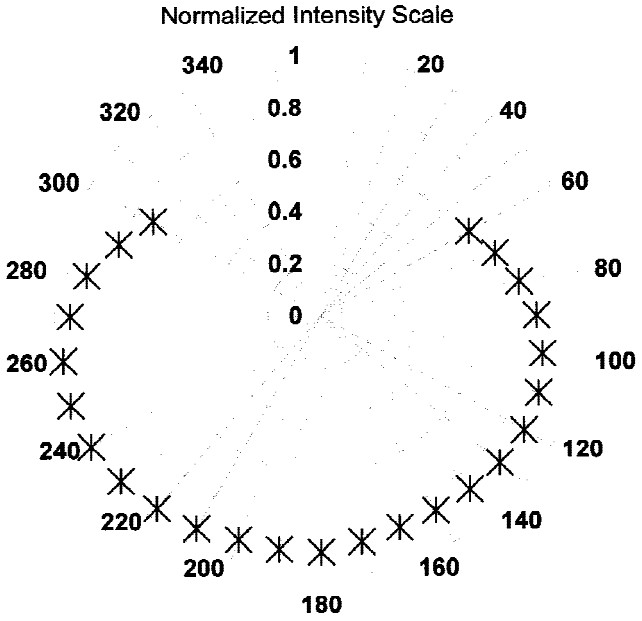

Fig. 9. Normalized detected fluence of dosimetry probe. Irradiation by an external collimated beam. The probe faces forward at 180°.